

The Dependence of the Solid State Structures of Bisparaphenylene-(3n+4)-crown-n Ethers upon Macrocyclic Ring Size

Alexandra M. Z. Slawin,^a Neil Spencer,^b J. Fraser Stoddart,^b and David J. Williams^a

^a Department of Chemistry, Imperial College, London SW7 2AY, U.K.

^b Department of Chemistry, The University, Sheffield S3 7HF, U.K.

X-Ray crystallography on the free BPP(3n+4)Cn ethers where $n = 7, 8, 10, 11,$ and 12 reveals a conformational dependence for the macrocycles which is reflected in their cavity sizes, with a maximum for $n = 10$, and in the relative orientations of the two hydroquinol rings, almost orthogonal for $n = 7$ and parallel or nearly parallel for $n = 8, 10, 11,$ and 12 , with respect to each other.

In the two preceding communications, the observation^{1,2} that [Diquat][PF₆]₂ and [Paraquat][PF₆]₂ form stable complexes with macrocyclic polyethers of the general type bisparaphenyl-

ene-(3n+4)-crown-n [BPP(3n+4)Cn][†] where $n = 8-12$ in solution, and where $n = 9$ and 10 in the solid state, together with the realisation³ that the free BPP34C10 receptor supports

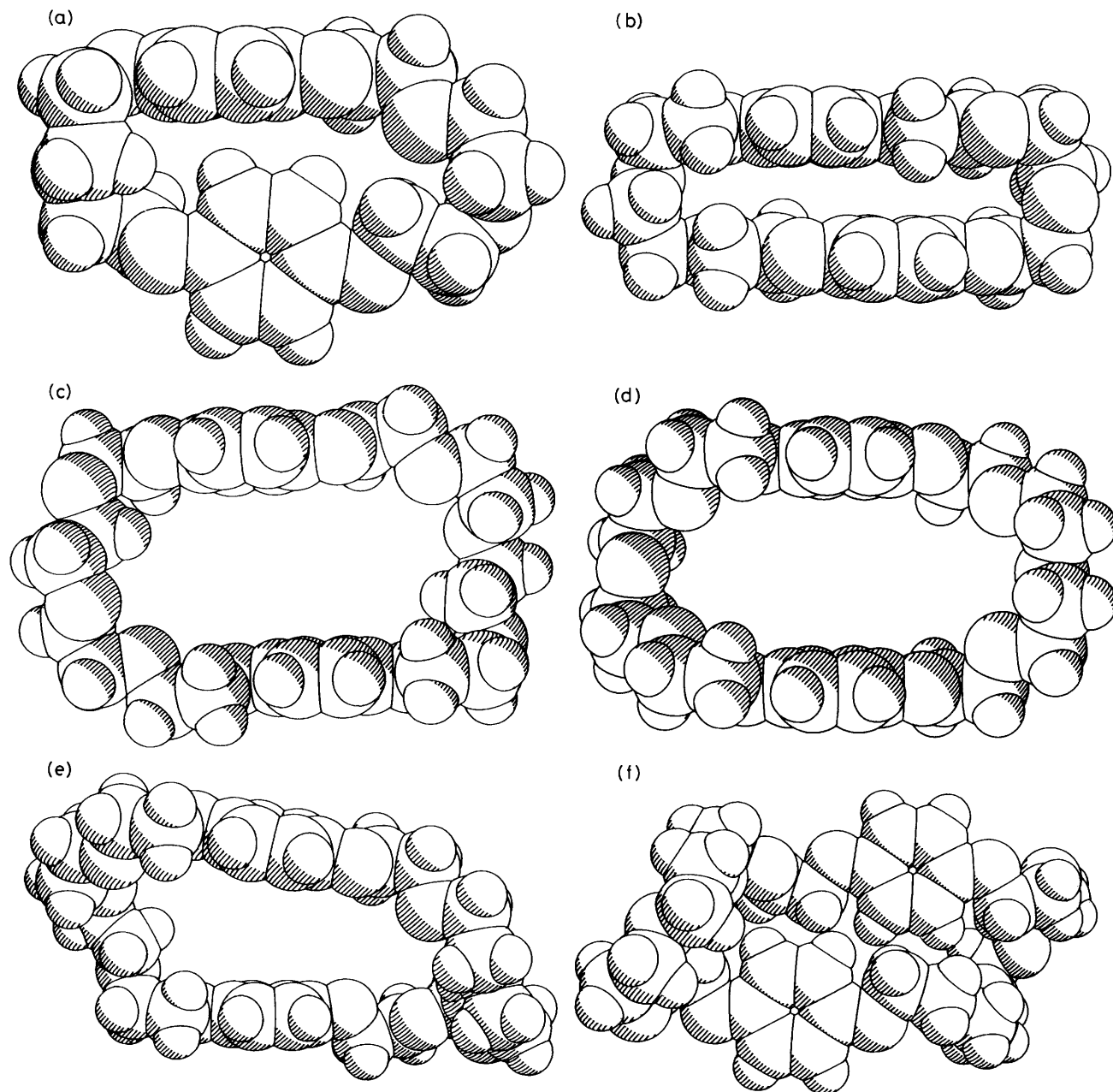


Figure 1. Space filling representations of (a) BPP25C7, (b) BPP28C8, (c) BPP34C10 [conformation (I)], (d) BPP34C10 [conformation (II)], (e) BPP37C11, and (f) BPP40C12. In (c) and (d), the distances between the centroids of the aromatic rings are 7.50 and 7.53 Å, respectively.

a large molecular cavity of approximately rectangular shape ($\sim 4.7 \times 10.6 \text{ \AA}$), prompted us to examine how the conformational features of the free BPP($3n + 4$) C_n receptors relate to the macrocyclic ring size across the series $n = 7-12$. Here, we present the *X*-ray crystal structures[†] of BPP25C7, BPP28C8, BPP37C11, and BPP40C12 and describe the differences in their gross conformational features and compare them with those³ of BPP34C10.

Figure 1 depicts space-filling representations[§] of the five BPP($3n+4$) C_n macrocycles[¶] for which crystal structures[‡] (Figures 2–5) have been determined.³ On progressing from the optimum receptor,¹ namely BPP34C10 (Figures 1c and 1d), for the [Paraquat]²⁺ dication, we see (Figures 1e and 1f) that, when the macrocyclic ring size increases in keeping with $n = 11$ and 12, the receptor cavity collapses progressively. Initially, a sizeable void is retained in BPP37C11 (Figure 1e) though there is noticeable tilting (16°) of one of the hydroquinol units with respect to the other. This situation may be compared with the parallel disposition of these units observed³ in both independent crystalline forms of BPP34C10 (Figures 1c and 1d). In the next higher homologue ($n = 12$), the filling of this cavity is complete with two hydroquinol rings in BPP40C12 (Figure 1f) becoming once again parallel but displaced laterally with respect to each other. On moving to the smaller homologues ($n = 7$ and 8), the cavity, as expected, contracts but displays dramatic conformational changes in the process. In BPP28C8 (Figure 1b), the parallel arrangement of

[†] The structural formulae for the BPP($3n+4$) C_n ethers are illustrated in the preceding communication (ref. 1) along with the syntheses of BPP25C7, BPP28C8, BPP37C11, and BPP40C12, and the solvents used in each case to grow single crystals suitable for *X*-ray crystallography.

[‡] *Crystal data* for BPP25C7: $C_{22}H_{28}O_7$, $M = 404.5$, triclinic, space group $P\bar{1}$, $a = 9.252(5)$, $b = 9.515(3)$, $c = 13.947(3) \text{ \AA}$, $\alpha = 70.65(2)$, $\beta = 72.31(3)$, $\gamma = 65.72(3)^\circ$, $U = 1036 \text{ \AA}^3$, $Z = 2$, $D_c = 1.30 \text{ g cm}^{-3}$, $\mu(\text{Cu-K}\alpha) = 8 \text{ cm}^{-1}$. The structure was solved by direct methods and refined anisotropically to give $R = 0.052$, $R_w = 0.072$ for 2013 independent observed reflections [$|F_o| > 3\sigma(|F_o|)$, $\theta \leq 50^\circ$].

BPP28C8: $C_{24}H_{32}O_8$, $M = 448.5$, monoclinic, space group $P2_1/c$, $a = 11.089(3)$, $b = 5.094(1)$, $c = 19.915(5) \text{ \AA}$, $\beta = 94.04(2)^\circ$, $U = 1122 \text{ \AA}^3$, $Z = 2$, $D_c = 1.33 \text{ g cm}^{-3}$, $\mu(\text{Cu-K}\alpha) = 8 \text{ cm}^{-1}$. The structure was solved by direct methods and refined anisotropically to give $R = 0.057$, $R_w = 0.071$ for 1390 independent observed reflections [$|F_o| > 3\sigma(|F_o|)$, $\theta \leq 58^\circ$].

BPP37C11: $C_{30}H_{44}O_{11}$, $M = 580.7$, orthorhombic, space group $P2_1ab$, $a = 8.123(2)$, $b = 15.854(3)$, $c = 23.502(4) \text{ \AA}$, $U = 3027 \text{ \AA}^3$, $Z = 4$, $D_c = 1.27 \text{ g cm}^{-3}$, $\mu(\text{Cu-K}\alpha) = 8 \text{ cm}^{-1}$. The structure was solved by direct methods and refined anisotropically to give $R = 0.048$, $R_w = 0.051$ for 1849 independent observed reflections [$|F_o| > 3\sigma(|F_o|)$, $\theta \leq 58^\circ$].

BPP40C12: $C_{32}H_{48}O_{12}$, $M = 600.5$, triclinic, space group $P\bar{1}$, $a = 8.289(2)$, $b = 10.107(3)$, $c = 10.653(4) \text{ \AA}$, $\alpha = 69.05(3)$, $\beta = 89.56(3)$, $\gamma = 84.25(2)^\circ$, $U = 829 \text{ \AA}^3$, $Z = 1$, $D_c = 1.20 \text{ g cm}^{-3}$, $\mu(\text{Cu-K}\alpha) = 8 \text{ cm}^{-1}$. The structure was solved by direct methods and refined anisotropically to give $R = 0.047$, $R_w = 0.064$ for 1623 independent reflections [$|F_o| > 3\sigma(|F_o|)$, $\theta \leq 50^\circ$].

In all four cases, data were measured on a Nicolet R3m diffractometer with $\text{Cu-K}\alpha$ radiation (graphite monochromator) using ω -scans. Atomic co-ordinates, bond lengths and angles, and thermal parameters have been deposited at the Cambridge Crystallographic Data Centre. See Notice to Authors, Issue No. 1.

[§] Departures from the predominant coplanarity of phenoxymethylene units with respect to their hydroquinol rings occur (*cf.* refs. 1–3) in BPP37C11 once and in BPP25C7 twice.

[¶] It should be noted that, in all the constitutionally-symmetrical BPP($3n+4$) C_n ethers studied ($n = 8, 10, 12$), there are crystallographic centres of symmetry at the centres of the macrocycles.

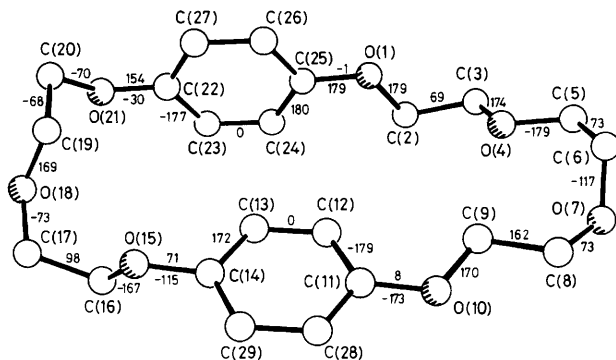


Figure 2. The solid state structure of BPP25C7. Torsional angles ($^\circ$) (O–C–C–O and C–C–O–C) associated with the two polyether chains are shown beside the relevant C–C and C–O bonds. The dihedral angle between the mean planes of the aromatic rings is 85° and the distance between their centroids is 5.03 \AA .

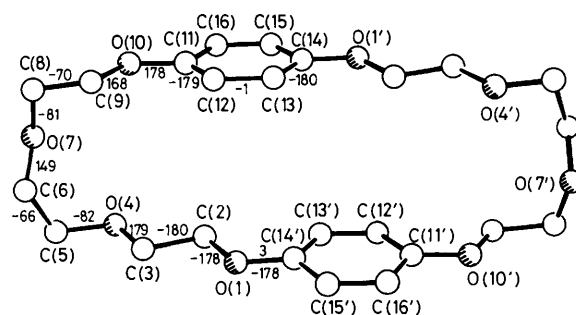


Figure 3. The solid state structure of BPP28C8. Torsional angles ($^\circ$) (O–C–C–O and C–C–O–C) associated with the symmetry-related polyether chains are shown beside the relevant C–C and C–O bonds in one of the chains. The aromatic rings are parallel and the distance between their centroids is 5.37 \AA .

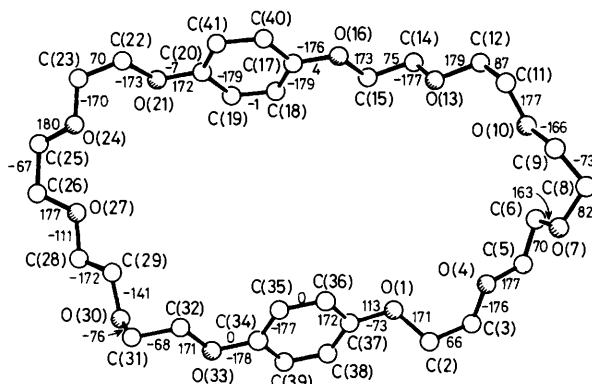


Figure 4. The solid state structure of BPP37C11. Torsional angles ($^\circ$) (O–C–C–O and C–C–O–C) associated with the two polyether chains are shown beside the relevant C–C and C–O bonds. The dihedral angle between the mean planes of the aromatic rings is 16° and the distance between their centroids is 8.05 \AA .

the hydroquinol rings is retained but the tendency seen³ in one (Figure 1c) of the two conformations of BPP34C10 for one of the rings to be displaced sideways with respect to the other is accentuated. The most pronounced conformational change occurs in BPP25C7 (Figure 1a) when the ring size is reduced

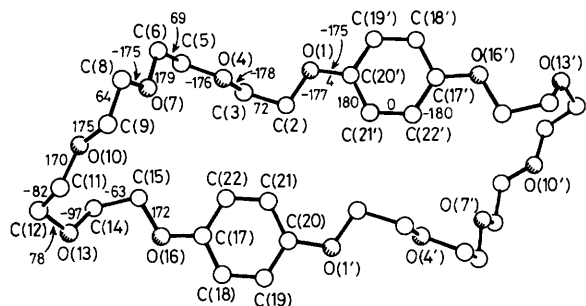


Figure 5. The solid state structure of BPP40C12. Torsional angles ($^{\circ}$) (O-C-O and C-C-O-C) associated with the symmetry-related polyether chains are shown beside the relevant C-C and C-O bonds in one of the chains. The aromatic rings are parallel and the distance between their centroids is 7.01 Å.

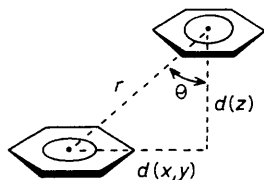


Figure 6. A schematic representation of two interacting benzene rings defining r , $d(x,y)$, $d(z)$, and θ .

further in accordance with $n = 7$; the preference for a parallel arrangement of the hydroquinol rings vanishes and they adopt a nearly orthogonal (85° between their mean planes) relationship. The conformational preferences displayed by BPP28C8

and BPP25C7 are consistent with recently reported⁴⁻⁶ analyses of the interaction geometries of aromatic amino acid side chains in proteins. Here, we see examples of conformations that match both the local (BPP28C8) and global (BPP25C7) potential energy minima identified theoretically⁵ for two interacting benzene molecules and experimentally^{4,6} from X-ray crystal structure data for phenyl and substituted phenyl rings. Values (Figure 6) of r , $d(x,y)$, and $d(z)$ are 5.4, 3.6, and 4.0 Å with $\theta = 42^{\circ}$ for BPP28C8 and 5.0, 1.1, and 4.9 Å with $\theta = 12^{\circ}$ for BPP25C7. These observed parameters are in close agreement with the values reported^{5,6} for local and global potential energy minima corresponding respectively to two face-to-face stacked and two edge-to-face stacked benzene rings. In the latter case, the $\delta(+)$ hydrogen, H(13), is directed into the centre of the $\delta(-)$ π -electron cloud of the C(22)-C(27) benzene ring with a distance of 2.8 Å from its centroid to H(13).

We acknowledge financial support for this research from A.F.R.C., S.E.R.C., and the Leverhulme Trust.

Received, 11th February 1987; Com. 190

References

- 1 B. L. Allwood, N. Spencer, H. Shahriari-Zavareh, J. F. Stoddart, and D. J. Williams, communication preceding the previous one.
- 2 P. R. Ashton, A. M. Z. Slawin, N. Spencer, J. F. Stoddart, and D. J. Williams, preceding communication.
- 3 B. L. Allwood, N. Spencer, H. Shahriari-Zavareh, J. F. Stoddart, and D. J. Williams, third communication in this series.
- 4 S. K. Burley and G. A. Petsko, *Science*, 1985, **229**, 23, and references therein.
- 5 S. K. Burley and G. A. Petsko, *J. Am. Chem. Soc.*, 1986, **108**, 7995.
- 6 R. O. Gould, A. M. Gray, P. Taylor, and M. D. Walkinshaw, *J. Am. Chem. Soc.*, 1985, **107**, 5921.